

Multi-Cue Adaptive Visual Token Pruning for Large Vision-Language Models

Bozhi Luan¹ Wengang Zhou¹ Hao Feng¹ Zhe Wang² Xiaosong Li² Houqiang Li¹

¹ University of Science and Technology of China, ² Huawei Technologies

{bzluan,haof}@mail.ustc.edu.cn, {zhwg,lihq}@ustc.edu.cn, {wangzhe226,lixiaosong20}@huawei.com

Abstract

As the computational needs of Large Vision-Language Models (LVLMs) increase, visual token pruning has proven effective in improving inference speed and memory efficiency. Traditional pruning methods in LVLMs predominantly focus on attention scores to determine token relevance, overlooking critical aspects such as spatial position and token similarity. To this end, we introduce AdaptPrune, a novel plug-and-play training-free pruning method that builds on conventional attention-based pruning by integrating spatial distance and token similarity with an adaptive NMS approach. Our method is based on several observed phenomena in large models: the positional bias in the model’s image attention and the redundancy of token information ignored by previous approaches. By integrating attention, spatial, and similarity information, our approach ensures a comprehensive evaluation of token importance and substantially refines the pruning decisions. Our method has been extensively tested across various LVLMs and benchmarks, confirming its robustness and adaptability. The results demonstrate that AdaptPrune consistently outperforms existing methods across various pruning ratios. Code is available at <https://github.com/bzluan/AdaptPrune>.

1. Introduction

Breakthroughs in Large Language Models (LLMs) [3, 12, 47] have revolutionized natural language processing with impressive performance across a diverse range of tasks [20, 50]. Building upon these advancements, Large Vision-Language Models (LVLMs) [29, 30] extend LLMs by converting images into hundreds or thousands of sequential visual representations and combined with text prompts. With the advancement of powerful visual understanding and question-answering capabilities, there has also been a rapid increase in computational complexity and memory usage.

A pioneering study FastV [9] has highlighted that while image tokens account for the majority of computational load, they receive far less attention than text tokens in

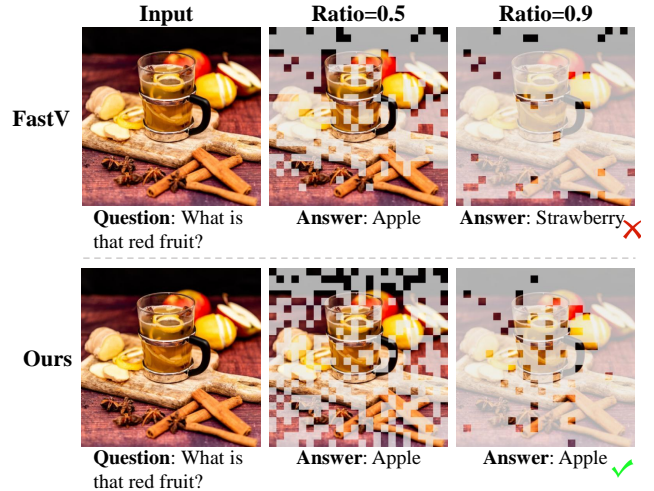


Figure 1. Comparison between FastV [9] and our AdaptPrune at different pruning ratios. FastV [9] utilizes only attention scores for token pruning, while AdaptPrune incorporates attention, spatial, and similarity information for a more holistic investigation.

the deeper layers of Large Vision-Language Models. A phenomenon known as “attention anchoring” [9, 52] has also been identified, where attention becomes concentrated on just a few specific image tokens, leaving most tokens with substantially reduced focus. Quantitative analyses in some studies [26, 55] further demonstrate that core attention points show minimal variation across layers and generation steps, reinforcing this observation.

Based on the above insights, some methods [9, 53, 55, 58] have been developed to prune image tokens with low attention scores at specific layers, reducing the computational load to accelerate inference while minimizing the impact on accuracy. Image tokens are re-evaluated based on their average received attention scores. Tokens falling below a predefined attention score threshold are then selectively discarded in subsequent layers, streamlining the process by focusing on the most impactful tokens. They not only bypass the computational demand of the self-attention module but also the Feed-Forward Network (FFN) module in deeper layers.

However, these pruning techniques are typically constrained to around 50% token reduction, as further pruning

often results in substantial performance degradation across tasks. As shown in Figure 1, we demonstrate that attention-only methods represented by FastV [9] have a tendency to keep tokens corresponding to the lower part of the image and often select clusters of tokens with high similarity. Our in-depth analysis of image tokens has highlighted two primary issues that constrain current attention-based pruning methods: positional bias of image attention and information redundancy in similar image tokens. These factors become especially problematic when aiming for more aggressive token pruning, and sharply degrading model performance.

To address these challenges, we propose AdaptPrune, a pioneering training-free pruning method for image tokens that incorporates three critical cues: attention scores, spatial positions, and token similarity. As depicted by the comparison in Figure 1, in contrast to FastV’s tendency to preserve clusters of similar tokens and focus on the lower part of the image, our AdaptPrune selects tokens that better represent diverse semantic regions for more information.

We innovatively reframe the visual token pruning problem as a Non-Maximum Suppression (NMS) task. Drawing inspiration from studies in the object detection area [5, 21, 31, 32], we treat each token as a candidate “detection” point, where its importance score reflects confidence and similarity indicates information density. AdaptPrune builds on attention scores and develops an adaptive NMS approach, suppressing tokens within a specified range based on spatial distance and token similarity. Our method initiates token pruning from a single layer, applying the pruning strategy consistently across subsequent layers and tokens without further adjustments to avoid introducing additional factors that could affect pruning outcomes.

We validate our findings through comprehensive statistical and visual analyses. In our experiments, we experiment on 5 well-known LVLMS and evaluate our AdaptPrune on multiple tasks including Image Captioning, General VQA, Text-based VQA, and Multimodal Reasoning. Extensive experiments demonstrate that AdaptPrune effectively addresses previous limitations, significantly minimizing performance loss even at higher pruning ratios across diverse models and benchmarks.

We summarize our contributions as follows:

- We identify and analyze the positional bias and information redundancy phenomena in attention distribution, emphasizing that spatial information and token similarity are also needed for a more holistic strategy.
- We propose AdaptPrune, an effective plug-and-play visual token pruning method that reframes the problem as an adaptive NMS task, integrating three critical cues: attention score, spatial distance, and token similarity.
- We perform extensive experiments on diverse vision-language benchmarks based on different LVLMS to verify the effectiveness of our AdaptPrune.

2. Related Work

Large Vision-Language Models (LVLMS). By employing a cross-modal projector that aligns visual encoders [41] with Large Language Models [3, 8, 12–14, 42, 47], LVLMS effectively bridged visual and language understanding [29, 30, 62]. Despite their effectiveness in various vision-language tasks, LVLMS still encounter challenges such as detailed information understanding and hallucinations [56]. To address this, recent advancements focused on increasing image resolution [4, 10, 11], which greatly enhanced the performance on fine-grained tasks like TextVQA [45] and DocVQA [38]. However, these approaches substantially raised the number of image tokens, increasing from 576 in LLaVA-1.5 [30] to over 2,000 in LLaVA-NEXT [29] and even exceeding 10,000 in InternVL2 [10], resulting in significantly higher computational demands and memory usage. Even with the KV Cache increasing the speed of the decoding stage, the computational complexity still scales quadratically with the token length in the prefill stage. Consequently, research into the effective pruning of redundant visual tokens becomes essential for optimizing the efficiency of LVLMS in real-world applications.

Token Reduction. Recent advancements in adaptive attention have improved computational efficiency in LLMs by reducing redundant tokens dynamically [16, 23, 39, 46, 57]. StreamingLLM [52] retained fixed-position caches for long-context processing, while FastGen [17] adapted KV Cache management to retain important tokens based on recent attention patterns. H2O [61] and ScissorHands [34] further optimized inference by selectively pruning KV pairs and retaining tokens with consistently high attention. Many trainable methods [7, 15, 24, 27, 43, 44, 54] focused on visual token reduction in vision transformers [41] before image tokens are projected into LLMs. However, when directly applied to LVLMS without training, these methods lead to performance degradation because they fail to incorporate LLM’s understanding of the textual context.

FastV [9] proposed an image token pruning method for LVLMS to address inefficiencies in image attention. This method pruned tokens based on their attention scores starting from a specific layer and achieved minimal impact on overall performance. FastV [9] has been validated across various benchmarks and models, with additional solutions introduced ensuring compatibility with KV Cache. Later methods [2, 28, 35, 49, 53, 55, 58] explored dynamic pruning for each token or multi-layer pruning based on attention scores. Despite its widespread usage in existing methods, the ranking criteria for token pruning have received limited exploration, which we aim to further improve.

Unlike most methods developed after FastV, which focus on multilayer or dynamic pruning for different output tokens, we aim to explore a more fundamental and crucial aspect of token pruning which is the cues of token ranking.

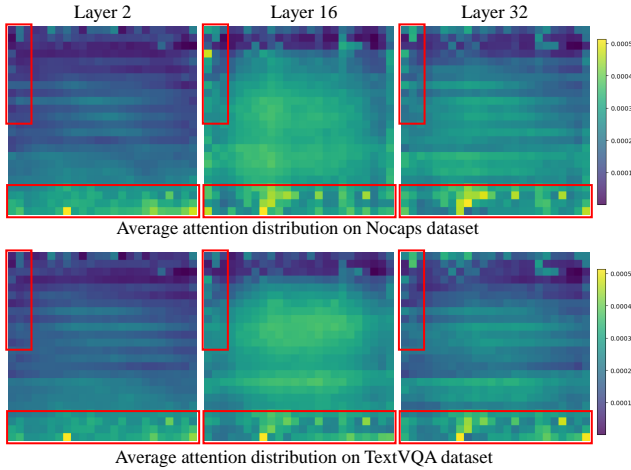


Figure 2. Visualization of attention positional bias phenomenon. The average attention distribution projected onto image patches exhibits a fixed pattern across different layers and tasks.

By addressing the phenomena we identified, We develop a more holistic ranking standard for visual token pruning. The detailed elaboration follows below.

3. Observations and Insights

In this section, we present several phenomena observed through experiments across different datasets. Prior work such as FastV [9] has revealed that image tokens constitute a substantial portion of input tokens, and they receive disproportionately less attention in deeper layers. Further studies [9, 26, 58, 60] have shown that the model consistently focuses on a subset of image tokens across multiple layers and generation steps. Building upon these significant findings, our experimental observations lead to new insights into the attention mechanisms of LVLMs, motivating us to propose strategies to improve token selection.

Positional Bias in Attention Distribution. As shown in Figure 2, we observe fixed motifs and patterns in the attention score distribution of image tokens which will cause positional bias in token pruning. We use 1000 samples from the Nocaps [1] dataset of the Image Captioning task and the TextVQA [45] dataset of the Text-based VQA task for statistics. Despite these samples coming from entirely different tasks, the model exhibits an almost identical attention distribution motifs for image tokens on the same layer. Across different layers, the shapes changes slightly but the tokens with the higher attention remain the same.

We observe that higher attention is distributed at the end of an image sequence. We interpret this phenomenon as a result of LVLMs inheriting the attention characteristics of their LLM component. Image patches are encoded as a token sequence and processed almost the same as a text paragraph during the pipeline of LVLMs. However, unlike text tokens, where boundary locations usually contain key infor-

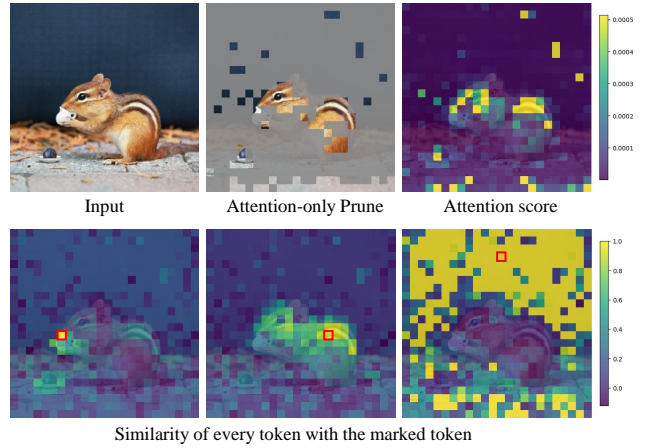


Figure 3. Visualization of the information redundancy phenomenon. The tokens with the highest attention score are kept, most of which are adjacent and have high similarity.

mation, the key information of an image is usually located in the central region [6]. Pruning methods that rely solely on attention scores [9, 53, 55, 58] tend to keep tokens in certain fixed positions and discard other essential tokens due to the bias of the model. As a result, such pruning strategies lead to performance degradation as the pruning ratio increases.

Information Redundancy in High Attention Tokens. When token selection relies solely on attention scores, the model tends to retain clusters of similar tokens, resulting in redundant information and inefficient use of computational resources. As shown in Figure 3, adjacent tokens with similar visual features in LVLMs often receive similar attention scores, particularly in areas with flat backgrounds or repetitive textures. Spatially close tokens capture overlapping features, making it difficult for the attention mechanism to differentiate unique or critical information. While attention-based pruning effectively captures central focus areas, it often overlooks important background context, leading to wasted attention on redundant information. To improve pruning efficiency and model performance, it is essential to incorporate similarity and informational uniqueness into the token selection process.

4. Method

As shown in Figure 4, our AdaptPrune reframes visual token pruning as a Non-Maximum Suppression (NMS) problem. Drawing inspiration from object detection [5, 31, 32], we treat each token as a candidate “detection” point with an importance score, which serves as a confidence measure. In our AdaptPrune, tokens with high similarity and proximity to the selected token are suppressed, retaining only diverse and essential information for downstream tasks. AdaptPrune optimizes inference by preserving token diversity and reducing redundancy, ultimately enhancing computational

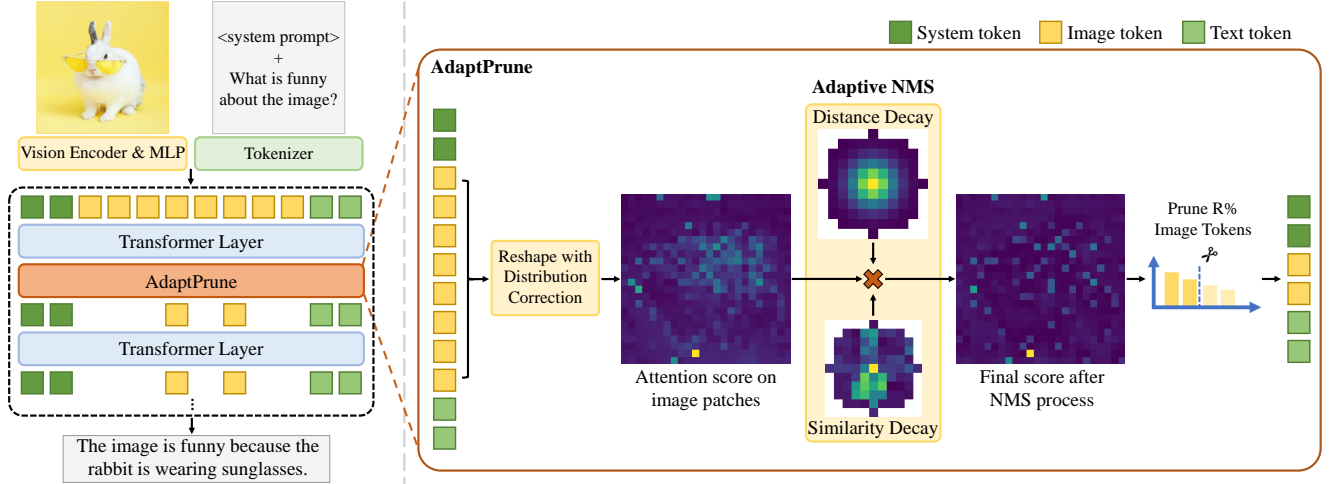


Figure 4. An overview of our AdaptPrune framework. AdaptPrune employs a simple and effective one-layer pruning strategy and incorporates an adaptive NMS algorithm to optimize the pruning process. AdaptPrune dynamically adjusts the suppression process using three critical cues: attention score, spatial distance, and token similarity.

efficiency without sacrificing model performance.

4.1. Distribution Correction

Based on our findings of attention’s positional bias, we propose adjusting the distribution of attention scores across image patches. Figure 8 of an influential study [6] points out that more information is distributed around the center of the image and suggests that the Gaussian function provides a good approximation. We apply a Gaussian mask centered at the image’s midpoint to the attention scores. This correction results in a more balanced attention distribution.

4.2. Factor Measurement

We employ three essential cues to calculate the scores of tokens in different aspects, explained below in terms of their measurement and computation.

Attention Scores Measurement. Like many existing methods [9], we utilize the attention values from the previous layer in the LVLm’s current token generation step to represent the importance of image tokens. This approach intuitively reflects the dependency of the current output token on all visual tokens and has been demonstrated by numerous prior studies to be an effective scoring mechanism.

Distance Measurement. Our method refines attention scoring by applying Soft NMS with two-dimensional spatial distance. To calculate this distance, we map image tokens back to their original patch positions. Unlike traditional NMS, which directly removes overlapping areas, Soft NMS gradually reduces scores based on token proximity, which prevents the forced removal of dense neighboring information. By leveraging a Gaussian decay function, we can control the range and intensity of distance suppression. This approach more efficiently chooses diverse regions across the

image to capture representative information.

Token Similarity Measurement. In high-resolution Text-based VQA benchmarks such as TextVQA [45] and DocVQA [38], answers are often concentrated in small, high-density regions, with each token representing unique details of the answer. This contrasts with tasks like Image Captioning or General VQA, which require broader contextual understanding. Drawing inspiration from the ZeroTPPrune [51] method, we incorporate token similarity as an additional filtering factor. By calculating the cosine similarity between key vectors, we implement an adaptive NMS that dynamically adjusts decay parameters based on both spatial distance and similarity. This adaptive pruning strategy effectively removes redundant tokens while retaining critical ones, enabling the model to better capture essential details at any density within the answer region.

4.3. Adaptive NMS

We propose an adaptive NMS algorithm suitable for candidate token selection in visual token pruning to integrate these three essential cues. At each iteration of the NMS process, we select the token t_i with the highest attention score s_i . For the currently selected token, we apply a suppression function to adjust the scores of nearby tokens t_j within a spatial range. The adaptive suppression function combines decay factors based on spatial distance and token similarity.

We compute the spatial decay function D_{spatial} and similarity decay function $D_{\text{similarity}}$ as follows:

$$D_{\text{spatial}} = \exp\left(-\frac{d(t_i, t_j)^2}{2\sigma_d^2}\right), \quad (1)$$

$$D_{\text{similarity}} = \exp\left(-\frac{(1 - \cos(\text{key}_i, \text{key}_j))^2}{2\sigma_s^2}\right). \quad (2)$$

The decay functions are calculated using spatial distance $d(t_i, t_j)$ and cosine similarity $\cos(\text{key}_i, \text{key}_j)$ between key vectors of the tokens, each modulated by decay factors σ_d and σ_s , respectively. The updated score s_j for each nearby token t_j is then calculated as:

$$s_j := s_j \cdot (1 - D_{\text{spatial}} \cdot D_{\text{similarity}}). \quad (3)$$

This function adaptively suppresses token scores using a multiplicative decay. Initial scores s_j are adjusted so that s_j reflects its spatial proximity and feature resemblance to t_i . This approach prioritizes spatially sparse tokens with distinct features, enhancing token selection flexibility through the adaptable decay parameters σ_d and σ_s .

At each step, we select the highest-scoring token that hasn’t yet been chosen and retain it. We then suppress the scores of surrounding tokens based on their spatial distance and similarity to the selected token. This iterative process continues until the pruning preservation ratio is met, with each newly selected token reducing the scores of its neighbors. This approach ensures that we retain only the most influential and representative tokens while effectively pruning those with redundant or less impactful information. Algorithm 1 shows the pseudocode for AdaptPrune.

4.4. Discussion

To summarize, our AdaptPrune introduces an advanced training-free token pruning strategy that unifies the cues of attention scores, spatial distance, and token similarity into cohesive importance ranking criteria of a balanced pruning approach. Applying AdaptPrune during the prefilling phase accelerates the prefilling speed while reducing the KV Cache length, which further enhances the decoding process. Our computational efficiency is almost identical to that of FastV [9], as both are single-layer pruning methods. Our adaptive strategy minimizes floating-point operations per second (FLOPs), effectively enhancing both inference speed and memory efficiency.

Unlike previous methods that primarily consider attention scores, AdaptPrune leverages spatial and similarity information to retain a more diverse token set, ensuring minimal impact on model accuracy even with substantial token reduction. By benefiting both the prefilling and decoding phases, this method offers a comprehensive optimization for long-context multimodal tasks, balancing memory efficiency and high-quality output retention.

5. Experiments

We evaluate the effectiveness of our method across 5 different models and 12 different benchmarks. We aim to provide

Algorithm 1 AdaptPrune

Require: Tokens T , scores S , positions P , keys K , distance decay parameter σ_d , similarity decay parameter σ_s , pruning ratio ratio .

Ensure: Retained tokens R .

```

1:  $R \leftarrow \emptyset$ ;
2:  $N \leftarrow \text{ratio} \times |T|$ ;
3:  $S \leftarrow \text{GaussianCorrection}(S, P)$ ;
4: while  $|R| < N$  do
5:    $i \leftarrow \arg \max_{k \in T} S[k]$ ;
6:    $R \leftarrow R \cup \{T[i]\}$ ;
7:   for  $j \in \text{Neighbors}(i)$  do
8:      $d \leftarrow \|P[i] - P[j]\|$ ;
9:      $\text{sim} \leftarrow \cos(K[i], K[j])$ ;
10:     $D_{\text{spatial}} \leftarrow \exp\left(-\frac{d^2}{2\sigma_d^2}\right)$ ;
11:     $D_{\text{similarity}} \leftarrow \exp\left(-\frac{(1-\text{sim})^2}{2\sigma_s^2}\right)$ ;
12:     $S[j] \leftarrow S[j] \cdot (1 - D_{\text{spatial}} \cdot D_{\text{similarity}})$ ;
13:   end for
14: end while
15: return  $R$ .
```

a comprehensive comparison of the performance of visual token pruning across diverse multimodal tasks.

5.1. Model Settings

For a fair comparison and efficient validation, we employ the LMMs-Eval [59] evaluation framework across all experiments. The models used include LLaVA-1.5 (7B and 13B variants) [29], LLaVA-NEXT-7B [10], and InternVL2 (2B and 8B variants) [10], with configurations based on their official settings. Detailed model architectures and settings are provided in the supplementary material.

5.2. Datasets

To demonstrate the broad applicability of our approach, we use several representative benchmark datasets that cover a wide spectrum of task domains for evaluation, including Nocaps [1] and Flickr30K [40] for Image Captioning, VQAv2 [18], GQA [22], OK-VQA [36] and VizWiz [19] for General Visual Question Answering, TextVQA [45], ChartQA [37] and DocVQA [38] for Text-based Visual Question Answering and POPE [25], MME and MMBench-EN [33] for Multimodal Reasoning. Detailed descriptions of the datasets and corresponding evaluation metrics are provided in the supplementary material.

5.3. Main Results

We begin by comparing the pruning result of FastV [9] and AdaptPrune across 5 LVLMs and 12 benchmarks at a high pruning ratio. Then we show experiments with various pruning ratios and qualitative visualizations to showcase the

Method	Image Caption		General VQA				Text-based VQA			Multimodal Reasoning		
	Nocaps	Flickr30K	VQAv2	GQA	OK-VQA	VizWiz	TextVQA	ChartQA	DocVQA	POPE	MME	MMB
LLaVA-1.5-7B [29]	105.8	75.2	76.6	61.9	53.4	54.2	45.9	18.1	28.1	87.0	1508.2	64.1
+ VTW [28] (K=5)	6.1	6.9	42.7	39.5	20.0	50.3	8.1	11.6	10.5	46.0	635.5	21.0
+ FastV [9]	74.2	47.4	63.8	51.0	43.9	54.9	38.5	14.6	18.0	69.7	1217.8	58.6
+ AdaptPrune	99.3	70.5	72.3	58.0	49.1	55.9	40.1	17.0	19.4	79.3	1393.2	59.4
LLaVA-1.5-13B [29]	109.4	79.5	79.2	63.3	58.3	56.6	48.7	18.1	30.3	87.1	1528.8	68.7
+ VTW [28] (K=5)	5.0	4.8	47.0	39.7	22.4	50.2	8.2	13.2	11.0	50.0	623.7	22.4
+ FastV [9]	94.6	65.4	68.7	54.6	51.4	57.2	38.3	15.2	17.5	74.8	1353.4	63.3
+ AdaptPrune	103.8	75.2	73.5	57.9	53.1	57.9	42.0	15.4	19.8	80.5	1461.2	65.1
LLaVA-NEXT-7B [29]	88.3	68.4	81.8	64.2	44.2	60.6	64.8	54.8	74.4	87.6	1519.5	67.2
+ FastV [9]	72.7	52.2	71.3	56.6	38.3	57.4	48.2	30.0	36.8	79.7	1352.7	61.3
+ AdaptPrune	82.1	61.7	76.7	59.6	41.0	58.9	55.8	33.8	45.0	84.3	1428.3	63.0

Table 1. Experiments on LLaVA with 90% pruning ratio for visual tokens. Under this experiment setting, the FLOPs of the LLaVA-1.5 [29] baseline model are reduced by around 81%, while the FLOPs of the LLaVA-NEXT [29] baseline model are reduced by around 87%.

Method	General VQA				Text-based VQA			Multimodal Reasoning		
	VQAv2	GQA	OK-VQA	VizWiz	TextVQA	ChartQA	DocVQA	POPE	MME	MMB
InternVL2-2B [10]	74.7	59.9	43.6	46.1	72.7	74.9	87.4	89.0	1444.6	72.3
+ FastV [9]	64.3	50.9	37.1	42.8	49.9	17.9	28.0	80.1	1339.3	65.2
+ AdaptPrune	66.5	52.1	39.2	44.2	52.7	22.8	31.1	82.5	1313.5	68.2
InternVL2-8B [10]	78.9	62.7	52.2	61.0	77.0	82.4	92.0	87.9	1628.7	82.0
+ FastV [9]	67.4	53.6	45.3	58.2	55.7	28.2	33.8	79.6	1510.0	71.2
+ AdaptPrune	71.6	55.7	47.5	59.9	57.4	32.8	42.9	82.1	1516.7	75.6

Table 2. Experiments on InternVL with 90% pruning ratio for visual tokens. InternVL [10] model FLOPs are reduced by around 88%.

pruning effects of our method. To ensure a fair comparison, we align key variables such as the pruning layer and pruning ratio across both methods. Specifically, the pruning layer is set to 3 following the optimal setup of FastV [9].

Comparison on 90% Pruning Ratio. As shown in Tables 1, 2 and 3, we evaluate 5 LVLMs using VTW [28], FastV [9] and AdaptPrune. Since AdaptPrune introduces a new ranking criterion in token selection process, we compare its single-layer pruning performance with FastV and VTW [28] for a fair evaluation. The evaluated LVLMs differ in model size, training data, and architecture. Since the InternVL2 [10] framework does not include Image Captioning tasks with CIDEr score [48], we omit those results. To assess method resilience, we select a 90% pruning ratio to test token pruning effectiveness, emphasizing AdaptPrune’s ability to maintain performance with minimal token retention, unlike FastV, which struggles with aggressive pruning.

Our method outperforms FastV across all models and benchmarks. Unlike previous attention-only methods that suffer performance drops at high pruning ratios, our approach minimizes loss even under aggressive pruning.

Experiments on Nocaps [1], Flickr30k [40], and General VQA benchmarks show that our method retains more informative tokens, preserving broader image content. As

shown in Figure 5 and 6, while FastV [9] suffers significant losses in image semantic information under extreme pruning, our analysis suggests that the semantic loss primarily stems from suboptimal ranking functions. Many non-informative tokens are included in the retained token set and genuinely informative tokens are filtered out, which causes the main performance decline. Our new pruning strategy selects a more informative and representative token set and preserves a wider array of image information.

For Text-based VQA benchmarks like TextVQA [45], DocVQA [38], and ChartQA [37], where answers are often confined to small, information-dense regions, the pruning algorithm must measure token density and redundancy. This necessitates that the pruning algorithm should effectively measure both the density and redundancy of token information. By incorporating token similarity into our AdaptPrune, we dynamically control the suppression degree, adjusting to varying levels of information clustering and redundancy. This demonstrates the effectiveness of the AdaptPrune strategy in leveraging multiple pruning cues to preserve model performance across various conditions.

Comparison at Different Pruning Ratios. As shown in Figure 5 We conduct experiments across a range of token pruning ratios, from 0.5 to 0.95, to evaluate how well our

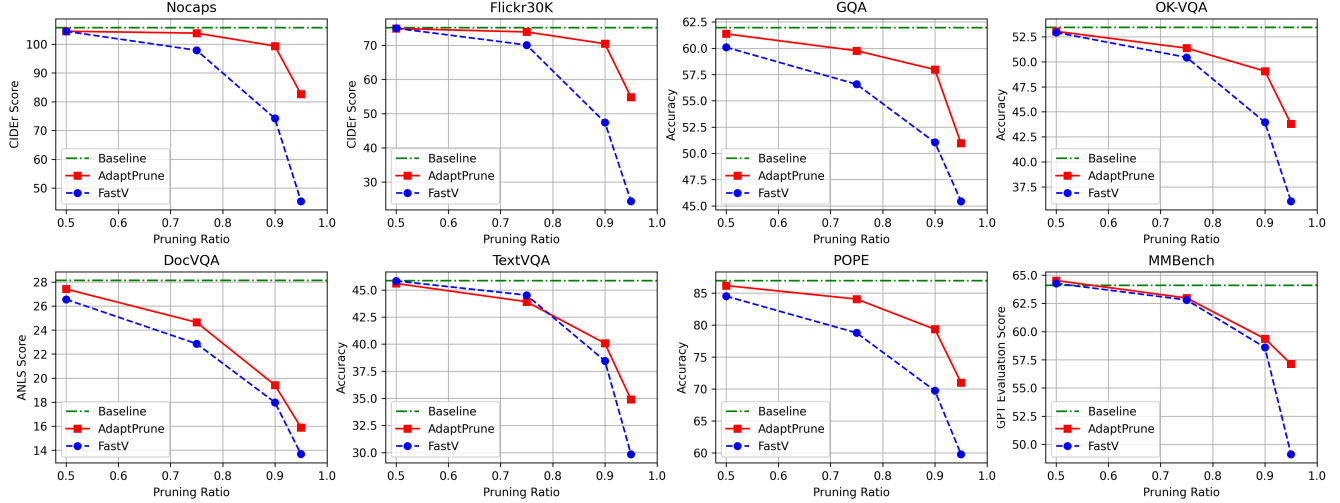


Figure 5. Performance comparison of FastV [9] and AdaptPrune on the LLaVA-1.5-7B model at different pruning ratios across eight evaluation benchmarks. The green line represents the LLaVA-1.5-7B baseline results without pruning.

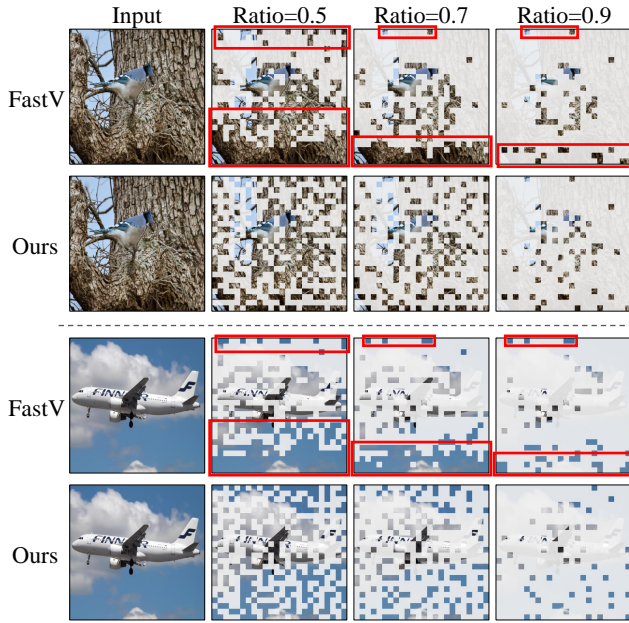


Figure 6. Visualization comparison between FastV [9] and our AdaptPrune on LLaVA-1.5-7B [29] at different pruning ratios of samples from Nocaps (upper) and TextVQA (lower). FastV’s redundant tokens at fixed positions are marked with red bboxes.

method maintains model performance at varying levels of token retention. By testing across these ratios, we aim to understand not only the robustness of our approach under different pruning intensities but also its adaptability across models and benchmarks. Unlike prior approaches that show steep performance degradation as pruning becomes more aggressive, our method demonstrates flexibility by preserving key image semantic information, even at high pruning ratios. This suggests that our method can dynamically ad-

Method	Time	GPU-Memory	Score	Latency
LLaVA-1.5-7B [29]	49:05	19G	87.0	0.327s
+ FastV [9]	27:30	14.4G	69.7	0.182s
+ AdaptPrune	31:25	14.5G	79.3	0.209s

Table 3. Real inference comparison on POPE dataset where the output is only one token. Experiments are on LLaVA-1.5-7B [29] on single 3090 GPU with the pruning ratio of 90%.

just to different levels of token sparsity, maintaining the quality of outputs while improving efficiency.

Qualitative Comparison. As shown in Figure 6, to gain deeper insights into the behavior of our method, we conduct a detailed visualization analysis using the LLaVA-1.5-7B model across all benchmarks. By sampling 1,000 images, we can examine token selection and pruning patterns in a more granular way. This analysis reveals how our approach differs from previous methods in selecting informative tokens and filtering out redundant ones. Specifically, we observe that our method consistently retains tokens that capture critical spatial and semantic details, leading to richer and more contextually accurate outputs. These visual comparisons illustrate how our adaptive token pruning strategy enhances model efficiency without compromising on the essential information needed for high-quality predictions.

5.4. Ablation Studies

To validate the effectiveness across the factors we introduced in our AdaptPrune, we conduct in-depth ablation experiments as detailed in Table 4 and 5. All ablation experiments are conducted on LLaVA-1.5-7B and the performance is assessed across benchmarks from different tasks.

Impact of Distribution Correction. We first evaluate a simplified variant (Table 4 (b)) of our AdaptPrune, where

Method	Correction	Distance	Similarity	Nocaps	Flickr30K	GQA	OK-VQA	DocVQA	TextVQA	POPE	MMB
LLaVA-1.5-7B [29]				105.8	75.2	61.9	53.4	28.1	45.9	87.0	64.1
(a)				74.2	47.5	51.0	43.9	18.0	38.5	69.7	58.6
(b)	✓			95.9	68.8	55.4	48.2	18.2	37.5	77.9	59.8
(c)	✓	✓		98.9	70.0	56.2	47.1	17.3	36.9	78.8	60.1
(d)	✓	✓	✓	99.3	70.5	58.0	49.1	19.4	40.1	79.3	59.4

Table 4. Ablation study across factors introduced in our AdaptPrune. Method (a) represents FastV [9] and the term ‘‘Correction’’ stands for our Distribution Correction operation. Experiments are conducted on LLaVA-1.5-7B [29] with the pruning ratio of 90%.

Method	GQA	OK-VQA	TextVQA	MMB
LLaVA-1.5-7B [29]	61.9	53.4	45.9	64.1
+ FastV [9]	51.0	43.9	38.5	58.6
+ AdaptPrune	58.0	49.1	40.1	59.4
(a) + FitPrune [55]	45.9	32.3	27.0	47.3
(b) + Skip	54.7	45.4	35.3	59.1
(c) + Random	56.0	40.0	20.2	56.7
(d) + Random 3x3	56.2	42.2	22.7	56.2
(e) + Max-pooling 3x3	56.0	47.7	33.2	58.9
(f) + Average-pooling	48.4	38.1	32.1	54.7
(g) + The last 10%	41.3	18.6	9.2	27.5

Table 5. Ablation study on alternative pruning strategies. Experiments are on LLaVA-1.5-7B [29] with the pruning ratio of 90%.

we only apply a Distribution Correction process to minimize the positional bias effect we observed. Following this correction, we prune tokens based on the adjusted attention scores. Compared with FastV [9] that used the attention score directly (Table 4 (a)), this approach improves performance across all benchmarks. This validates our observation that the model’s positional attention bias phenomenon. The biased attention distribution does not accurately reflect the true importance of information. The performance improvements across all benchmarks demonstrate that the Distribution Correction process allows new scores to more accurately represent the importance of visual information.

Impact of Distance Decay. Based on the simplified variant (Table 4 (b)), we further introduce the distance decay to reduce the redundancy (Table 4 (c)). We observed that the selected tokens tend to cluster together, which usually means the information is highly similar. To address this, we incorporate the distance factor into our attention-based pruning strategy using a Soft NMS approach. This method suppresses the scores of tokens in the surrounding area of each selected token based on their distance, effectively promoting a more even token distribution across the image. Experiment results show significant performance improvements in Image Captioning, General VQA, and Multimodal Reasoning tasks. However, on Text-based VQA benchmarks TextVQA [45] and DocVQA [38], performance is below the attention-only approach of FastV [9]. We at-

tribute this to the enforced spatial dispersion of selected tokens, which leads to information loss in tasks where answers are concentrated in very small regions.

Impact of Similarity Decay. To accommodate tasks with varying information densities, we integrate similarity information into our method (Table 4 (d)). To ensure each retained token represents distinct information, we adjust the decay effect on neighboring tokens based on the similarity of their key vectors. Thus we propose the full version of our AdaptPrune approach. AdaptPrune suppresses the surrounding tokens’ attention score of the selected tokens with distance and similarity information. Experimental results show that our AdaptPrune consistently outperforms FastV [9] across all tasks and achieves the best performance compared to incomplete versions on almost all benchmarks.

Comparison with Alternative Pruning Strategy. As shown in Table 5, we experimented with alternative scoring and pruning strategies under our framework to validate the effectiveness of our method. We performed a comprehensive comparison with methods such as average pooling, max pooling, and random selection, with the specific implementations detailed in the supplementary material. The experimental results demonstrate that our method achieves the highest performance at the same pruning ratio.

6. Conclusion

In this paper, we introduce AdaptPrune, a novel training-free token pruning method designed to enhance the efficiency of Large Vision-Language Models (LVLMs). Our method addresses the key limitations of existing token pruning strategies, which predominantly rely on attention scores alone. By incorporating spatial information and token similarity, AdaptPrune provides a more holistic approach to token selection, ensuring that redundant tokens are suppressed while retaining those that contribute to the model’s performance. Through extensive experiments across multiple models and benchmarks, we demonstrate that AdaptPrune significantly improves both speed and memory efficiency while maintaining minimal accuracy loss, even when pruning up to 90% of the tokens. Our results validate the importance of considering multiple cues of token relevance in optimizing the performance of multimodal models.

References

- [1] Harsh Agrawal, Karan Desai, Yufei Wang, Xinlei Chen, Rishabh Jain, Mark Johnson, Dhruv Batra, Devi Parikh, Stefan Lee, and Peter Anderson. Nocaps: Novel object captioning at scale. In *Proceedings of the IEEE/CVF International Conference on Computer Vision*, pages 8948–8957, 2019. [3](#), [5](#), [6](#), [1](#)
- [2] Kazi Hasan Ibn Arif, JinYi Yoon, Dimitrios S Nikolopoulos, Hans Vandierendonck, Deepu John, and Bo Ji. Hired: Attention-guided token dropping for efficient inference of high-resolution vision-language models in resource-constrained environments. *arXiv preprint arXiv:2408.10945*, 2024. [2](#)
- [3] Jinze Bai, Shuai Bai, Yunfei Chu, Zeyu Cui, Kai Dang, Xiaodong Deng, Yang Fan, Wenbin Ge, Yu Han, Fei Huang, et al. Qwen technical report. *arXiv preprint arXiv:2309.16609*, 2023. [1](#), [2](#)
- [4] Jinze Bai, Shuai Bai, Shusheng Yang, Shijie Wang, Sinan Tan, Peng Wang, Junyang Lin, Chang Zhou, and Jingren Zhou. Qwen-vl: A versatile vision-language model for understanding, localization, text reading, and beyond. *arXiv preprint arXiv:2308.12966*, 1(2):3, 2023. [2](#)
- [5] Navaneeth Bodla, Bharat Singh, Rama Chellappa, and Larry S Davis. Soft-nms—improving object detection with one line of code. In *Proceedings of the IEEE/CVF International Conference on Computer Vision*, pages 5561–5569, 2017. [2](#), [3](#)
- [6] Ali Borji and Laurent Itti. State-of-the-art in visual attention modeling. *IEEE Transactions on Pattern Analysis and Machine Intelligence*, 35(1):185–207, 2012. [3](#), [4](#)
- [7] Jieneng Chen, Luoxin Ye, Ju He, Zhao-Yang Wang, Daniel Khashabi, and Alan Yuille. Llavolta: Efficient multi-modal models via stage-wise visual context compression. *arXiv preprint arXiv:2406.20092*, 2024. [2](#)
- [8] Lin Chen, Jisong Li, Xiaoyi Dong, Pan Zhang, Conghui He, Jiaqi Wang, Feng Zhao, and Dahua Lin. Sharegpt4v: Improving large multi-modal models with better captions. *arXiv preprint arXiv:2311.12793*, 2023. [2](#)
- [9] Liang Chen, Haozhe Zhao, Tianyu Liu, Shuai Bai, Junyang Lin, Chang Zhou, and Baobao Chang. An image is worth 1/2 tokens after layer 2: Plug-and-play inference acceleration for large vision-language models. *arXiv preprint arXiv:2403.06764*, 2024. [1](#), [2](#), [3](#), [4](#), [5](#), [6](#), [7](#), [8](#)
- [10] Zhe Chen, Weiyun Wang, Hao Tian, Shenglong Ye, Zhangwei Gao, Erfei Cui, Wenwen Tong, Kongzhi Hu, Jiapeng Luo, Zheng Ma, et al. How far are we to gpt-4v? closing the gap to commercial multimodal models with open-source suites. *arXiv preprint arXiv:2404.16821*, 2024. [2](#), [5](#), [6](#), [1](#)
- [11] Zhe Chen, Jiannan Wu, Wenhui Wang, Weijie Su, Guo Chen, Sen Xing, Muyan Zhong, Qinglong Zhang, Xizhou Zhu, Lewei Lu, et al. Internvl: Scaling up vision foundation models and aligning for generic visual-linguistic tasks. In *Proceedings of the IEEE/CVF Conference on Computer Vision and Pattern Recognition*, pages 24185–24198, 2024. [2](#)
- [12] Wei-Lin Chiang, Zhuohan Li, Zi Lin, Ying Sheng, Zhanghao Wu, Hao Zhang, Lianmin Zheng, Siyuan Zhuang, Yonghao Zhuang, Joseph E Gonzalez, et al. Vicuna: An open-source chatbot impressing gpt-4 with 90%* chatgpt quality. See <https://vicuna.lmsys.org>, 2(3):6, 2023. [1](#), [2](#)
- [13] Wenliang Dai, Junnan Li, Dongxu Li, Anthony Meng Huat Tiong, Junqi Zhao, Weisheng Wang, Boyang Li, Pascale N Fung, and Steven Hoi. Instructblip: Towards general-purpose vision-language models with instruction tuning. *Proceedings of the Advances in Neural Information Processing Systems*, 36, 2024.
- [14] Jacob Devlin, Ming-Wei Chang, Kenton Lee, and Kristina Toutanova. Bert: Pre-training of deep bidirectional transformers for language understanding. *arXiv preprint arXiv:1810.04805*, 2018. [2](#)
- [15] Shuangrui Ding, Peisen Zhao, Xiaopeng Zhang, Rui Qian, Hongkai Xiong, and Qi Tian. Prune spatio-temporal tokens by semantic-aware temporal accumulation. In *Proceedings of the IEEE/CVF International Conference on Computer Vision*, pages 16945–16956, 2023. [2](#)
- [16] Qichen Fu, Minsik Cho, Thomas Merth, Sachin Mehta, Mohammad Rastegari, and Mahyar Najibi. Lazyllm: Dynamic token pruning for efficient long context llm inference. *arXiv preprint arXiv:2407.14057*, 2024. [2](#)
- [17] Suyu Ge, Yunan Zhang, Liyuan Liu, Minjia Zhang, Jiawei Han, and Jianfeng Gao. Model tells you what to discard: Adaptive kv cache compression for llms. *arXiv preprint arXiv:2310.01801*, 2023. [2](#)
- [18] Yash Goyal, Tejas Khot, Douglas Summers-Stay, Dhruv Batra, and Devi Parikh. Making the v in vqa matter: Elevating the role of image understanding in visual question answering. In *Proceedings of the IEEE/CVF Conference on Computer Vision and Pattern Recognition*, pages 6904–6913, 2017. [5](#), [1](#), [3](#), [4](#)
- [19] Danna Gurari, Qing Li, Abigale J Stangl, Anhong Guo, Chi Lin, Kristen Grauman, Jiebo Luo, and Jeffrey P Bigham. Vizwiz grand challenge: Answering visual questions from blind people. In *Proceedings of the IEEE/CVF Conference on Computer Vision and Pattern Recognition*, pages 3608–3617, 2018. [5](#), [1](#)
- [20] Dan Hendrycks, Collin Burns, Steven Basart, Andy Zou, Mantas Mazeika, Dawn Song, and Jacob Steinhardt. Measuring massive multitask language understanding. *arXiv preprint arXiv:2009.03300*, 2020. [1](#)
- [21] Jan Hosang, Rodrigo Benenson, and Bernt Schiele. Learning non-maximum suppression. In *Proceedings of the IEEE/CVF Conference on Computer Vision and Pattern Recognition*, pages 4507–4515, 2017. [2](#)
- [22] Drew A Hudson and Christopher D Manning. Gqa: A new dataset for real-world visual reasoning and compositional question answering. In *Proceedings of the IEEE/CVF Conference on Computer Vision and Pattern Recognition*, pages 6700–6709, 2019. [5](#), [1](#)
- [23] Huiqiang Jiang, Yucheng Li, Chengruidong Zhang, Qianhui Wu, Xufang Luo, Surin Ahn, Zhenhua Han, Amir H Abdi, Dongsheng Li, Chin-Yew Lin, et al. Miference 1.0: Accelerating pre-filling for long-context llms via dynamic sparse attention. *arXiv preprint arXiv:2407.02490*, 2024. [2](#)
- [24] Zhenglun Kong, Peiyan Dong, Xiaolong Ma, Xin Meng, Wei Niu, Mengshu Sun, Xuan Shen, Geng Yuan, Bin Ren,

- Hao Tang, et al. Spvit: Enabling faster vision transformers via latency-aware soft token pruning. In *Proceedings of the European Conference on Computer Vision*, pages 620–640. Springer, 2022. 2
- [25] Yifan Li, Yifan Du, Kun Zhou, Jinpeng Wang, Wayne Xin Zhao, and Ji-Rong Wen. Evaluating object hallucination in large vision-language models. *arXiv preprint arXiv:2305.10355*, 2023. 5, 2
- [26] Yuhong Li, Yingbing Huang, Bowen Yang, Bharat Venkitesh, Acyr Locatelli, Hanchen Ye, Tianle Cai, Patrick Lewis, and Deming Chen. Snapkv: Llm knows what you are looking for before generation. *arXiv preprint arXiv:2404.14469*, 2024. 1, 3
- [27] Youwei Liang, Chongjian Ge, Zhan Tong, Yibing Song, Jue Wang, and Pengtao Xie. Not all patches are what you need: Expediting vision transformers via token reorganizations. *arXiv preprint arXiv:2202.07800*, 2022. 2
- [28] Zhihang Lin, Mingbao Lin, Luxi Lin, and Rongrong Ji. Boosting multimodal large language models with visual tokens withdrawal for rapid inference. *arXiv preprint arXiv:2405.05803*, 2024. 2, 6
- [29] Haotian Liu, Chunyuan Li, Yuheng Li, and Yong Jae Lee. Improved baselines with visual instruction tuning. In *Proceedings of the IEEE/CVF Conference on Computer Vision and Pattern Recognition*, pages 26296–26306, 2024. 1, 2, 5, 6, 7, 8, 3
- [30] Haotian Liu, Chunyuan Li, Qingyang Wu, and Yong Jae Lee. Visual instruction tuning. *Proceedings of the Advances in Neural Information Processing Systems*, 36, 2024. 1, 2
- [31] Songtao Liu, Di Huang, and Yunhong Wang. Adaptive nms: Refining pedestrian detection in a crowd. In *Proceedings of the IEEE/CVF Conference on Computer Vision and Pattern Recognition*, pages 6459–6468, 2019. 2, 3
- [32] Wei Liu, Dragomir Anguelov, Dumitru Erhan, Christian Szegedy, Scott Reed, Cheng-Yang Fu, and Alexander C Berg. Ssd: Single shot multibox detector. In *Proceedings of the European Conference on Computer Vision*, pages 21–37. Springer, 2016. 2, 3
- [33] Yuan Liu, Haodong Duan, Yuanhan Zhang, Bo Li, Songyang Zhang, Wangbo Zhao, Yike Yuan, Jiaqi Wang, Conghui He, Ziwei Liu, et al. Mmbench: Is your multi-modal model an all-around player? In *Proceedings of the European Conference on Computer Vision*, pages 216–233. Springer, 2025. 5, 2, 3
- [34] Zichang Liu, Aditya Desai, Fangshuo Liao, Weitao Wang, Victor Xie, Zhaozhuo Xu, Anastasios Kyrillidis, and Anshumali Shrivastava. Scissorhands: Exploiting the persistence of importance hypothesis for llm kv cache compression at test time. *Proceedings of the Advances in Neural Information Processing Systems*, 36, 2024. 2
- [35] Zuyan Liu, Benlin Liu, Jiahui Wang, Yuhao Dong, Guangyi Chen, Yongming Rao, Ranjay Krishna, and Jiwen Lu. Efficient inference of vision instruction-following models with elastic cache. *arXiv preprint arXiv:2407.18121*, 2024. 2
- [36] Kenneth Marino, Mohammad Rastegari, Ali Farhadi, and Roozbeh Mottaghi. Ok-vqa: A visual question answering benchmark requiring external knowledge. In *Proceedings of the IEEE/CVF Conference on Computer Vision and Pattern Recognition*, pages 3195–3204, 2019. 5, 1
- [37] Ahmed Masry, Do Xuan Long, Jia Qing Tan, Shafiq Joty, and Enamul Hoque. Chartqa: A benchmark for question answering about charts with visual and logical reasoning. *arXiv preprint arXiv:2203.10244*, 2022. 5, 6, 2
- [38] Minesh Mathew, Dimosthenis Karatzas, and CV Jawahar. Docvqa: A dataset for vqa on document images. In *Proceedings of the IEEE/CVF Winter Conference on Applications of Computer Vision*, pages 2200–2209, 2021. 2, 4, 5, 6, 8
- [39] Shuai Peng, Di Fu, Baole Wei, Yong Cao, Liangcai Gao, and Zhi Tang. Vote&mix: Plug-and-play token reduction for efficient vision transformer. *arXiv preprint arXiv:2408.17062*, 2024. 2
- [40] Bryan A Plummer, Liwei Wang, Chris M Cervantes, Juan C Caicedo, Julia Hockenmaier, and Svetlana Lazebnik. Flickr30k entities: Collecting region-to-phrase correspondences for richer image-to-sentence models. In *Proceedings of the IEEE/CVF International Conference on Computer Vision*, pages 2641–2649, 2015. 5, 6, 1
- [41] Alec Radford, Jong Wook Kim, Chris Hallacy, Aditya Ramesh, Gabriel Goh, Sandhini Agarwal, Girish Sastry, Amanda Askell, Pamela Mishkin, Jack Clark, et al. Learning transferable visual models from natural language supervision. In *Proceedings of the International Conference on Machine Learning*, pages 8748–8763, 2021. 2
- [42] Colin Raffel, Noam Shazeer, Adam Roberts, Katherine Lee, Sharan Narang, Michael Matena, Yanqi Zhou, Wei Li, and Peter J Liu. Exploring the limits of transfer learning with a unified text-to-text transformer. *Journal of Machine Learning Research*, 21(140):1–67, 2020. 2
- [43] Yuzhang Shang, Mu Cai, Bingxin Xu, Yong Jae Lee, and Yan Yan. Llva-prumerge: Adaptive token reduction for efficient large multimodal models. *arXiv preprint arXiv:2403.15388*, 2024. 2
- [44] Dachuan Shi, Chaofan Tao, Anyi Rao, Zhendong Yang, Chun Yuan, and Jiaqi Wang. Crossget: Cross-guided ensemble of tokens for accelerating vision-language transformers. *arXiv preprint arXiv:2305.17455*, 2023. 2
- [45] Amanpreet Singh, Vivek Natarajan, Meet Shah, Yu Jiang, Xinlei Chen, Dhruv Batra, Devi Parikh, and Marcus Rohrbach. Towards vqa models that can read. In *Proceedings of the IEEE/CVF Conference on Computer Vision and Pattern Recognition*, pages 8317–8326, 2019. 2, 3, 4, 5, 6, 8
- [46] Dingjie Song, Wenjun Wang, Shunian Chen, Xidong Wang, Michael Guan, and Benyou Wang. Less is more: A simple yet effective token reduction method for efficient multimodal llms. *arXiv preprint arXiv:2409.10994*, 2024. 2
- [47] Hugo Touvron, Thibaut Lavril, Gautier Izacard, Xavier Martinet, Marie-Anne Lachaux, Timothée Lacroix, Baptiste Rozière, Naman Goyal, Eric Hambro, Faisal Azhar, et al. Llama: Open and efficient foundation language models. *arXiv preprint arXiv:2302.13971*, 2023. 1, 2
- [48] Ramakrishna Vedantam, C Lawrence Zitnick, and Devi Parikh. Cider: Consensus-based image description evaluation. In *Proceedings of the IEEE/CVF Conference on Computer Vision and Pattern Recognition*, pages 4566–4575, 2015. 6, 1

- [49] Zhongwei Wan, Ziang Wu, Che Liu, Jinfa Huang, Zhihong Zhu, Peng Jin, Longyue Wang, and Li Yuan. Look-m: Look-once optimization in kv cache for efficient multimodal long-context inference. *arXiv preprint arXiv:2406.18139*, 2024. [2](#)
- [50] Alex Wang. Glue: A multi-task benchmark and analysis platform for natural language understanding. *arXiv preprint arXiv:1804.07461*, 2018. [1](#)
- [51] Hongjie Wang, Bhishma Dedhia, and Niraj K Jha. Zero-tp prune: Zero-shot token pruning through leveraging of the attention graph in pre-trained transformers. In *Proceedings of the IEEE/CVF Conference on Computer Vision and Pattern Recognition*, pages 16070–16079, 2024. [4](#)
- [52] Guangxuan Xiao, Yuandong Tian, Beidi Chen, Song Han, and Mike Lewis. Efficient streaming language models with attention sinks. *arXiv preprint arXiv:2309.17453*, 2023. [1](#), [2](#)
- [53] Long Xing, Qidong Huang, Xiaoyi Dong, Jiajie Lu, Pan Zhang, Yuhang Zang, Yuhang Cao, Conghui He, Jiaqi Wang, Feng Wu, et al. Pyramidrop: Accelerating your large vision-language models via pyramid visual redundancy reduction. *arXiv preprint arXiv:2410.17247*, 2024. [1](#), [2](#), [3](#)
- [54] Yizhe Xiong, Hui Chen, Tianxiang Hao, Zijia Lin, Jun-gong Han, Yuesong Zhang, Guoxin Wang, Yongjun Bao, and Guiguang Ding. Pyra: Parallel yielding re-activation for training-inference efficient task adaptation. In *Proceedings of the European Conference on Computer Vision*, pages 455–473. Springer, 2025. [2](#)
- [55] Weihao Ye, Qiong Wu, Wenhao Lin, and Yiyi Zhou. Fit and prune: Fast and training-free visual token pruning for multi-modal large language models. *arXiv preprint arXiv:2409.10197*, 2024. [1](#), [2](#), [3](#), [8](#)
- [56] Shukang Yin, Chaoyou Fu, Sirui Zhao, Tong Xu, Hao Wang, Dianbo Sui, Yunhang Shen, Ke Li, Xing Sun, and Enhong Chen. Woodpecker: Hallucination correction for multimodal large language models. *arXiv preprint arXiv:2310.16045*, 2023. [2](#)
- [57] Gaotong Yu, Yi Chen, and Jian Xu. Balancing performance and efficiency: A multimodal large language model pruning method based image text interaction. *arXiv preprint arXiv:2409.01162*, 2024. [2](#)
- [58] Junyang Zhang, Mu Yuan, Ruiguang Zhong, Puhao Luo, Huiyou Zhan, Ningkan Zhang, Chengchen Hu, and Xiangyang Li. A-vl: Adaptive attention for large vision-language models. *arXiv preprint arXiv:2409.14846*, 2024. [1](#), [2](#), [3](#)
- [59] Kaichen Zhang, Bo Li, Peiyuan Zhang, Fanyi Pu, Joshua Adrian Cahyono, Kairui Hu, Shuai Liu, Yuanhan Zhang, Jingkang Yang, Chunyuan Li, et al. Lmms-eval: Reality check on the evaluation of large multimodal models. *arXiv preprint arXiv:2407.12772*, 2024. [5](#), [1](#)
- [60] Yichi Zhang, Bofei Gao, Tianyu Liu, Keming Lu, Wayne Xiong, Yue Dong, Baobao Chang, Junjie Hu, Wen Xiao, et al. Pyramidkv: Dynamic kv cache compression based on pyramidal information funneling. *arXiv preprint arXiv:2406.02069*, 2024. [3](#)
- [61] Zhenyu Zhang, Ying Sheng, Tianyi Zhou, Tianlong Chen, Lianmin Zheng, Ruisi Cai, Zhao Song, Yuandong Tian, Christopher Ré, Clark Barrett, et al. H2o: Heavy-hitter oracle for efficient generative inference of large language models. *Proceedings of the Advances in Neural Information Processing Systems*, 36, 2024. [2](#)
- [62] Deyao Zhu, Jun Chen, Xiaoqian Shen, Xiang Li, and Mohamed Elhoseiny. Minigt-4: Enhancing vision-language understanding with advanced large language models. *arXiv preprint arXiv:2304.10592*, 2023. [2](#)

Multi-Cue Adaptive Visual Token Pruning for Large Vision-Language Models

Supplementary Material

In the supplementary material, we provide detailed descriptions of the model architectures and settings, benchmark datasets along with their respective evaluation metrics, and alternative pruning strategies. Additionally, we present fine-grained results on the MMBench and MME benchmarks. We also offer visualization comparisons between FastV [9] and our AdaptPrune method at various pruning ratios, along with the average attention distribution across each layer of LLaVA-1.5-7B [29] on different datasets.

A. Model Settings

For a fair comparison and efficient validation, we employ the LMMs-Eval [59] evaluation framework across all experiments. The models used include LLaVA-1.5 (7B and 13B variants) [29], LLaVA-NEXT-7B [10], and InternVL2 (2B and 8B variants) [10]. We set the configurations based on their official settings.

LLaVA-1.5. The model architecture of LLaVA-1.5 [29] replaces the linear projection in LLaVA [30] with an MLP to map visual features into a shared embedding space with the language model. It uses CLIP-ViT-L as the visual encoder at a resolution of 336×336, with Vicuna as the language decoder. The image is divided into 24×24 patches, generating 576 image tokens. We implement our AdaptPrune by restoring the image sequences to a two-dimensional arrangement on LLaVA-1.5.

LLaVA-NEXT. LLaVA-NEXT [29] is an adaptive high-resolution model that divides input images into smaller grid patches, each encoded at the native resolution of 336×336, and then merges them into a large feature map. By removing image padding, it adjusts seamlessly to any aspect ratio. To add global context and reduce stitching artifacts, it also concatenates features from a downsampled image with the merged map, allowing efficient support for any resolution. Since the final image tokens are merged into two image sequences, we restore each image sequence to a two-dimensional arrangement and then perform our AdaptPrune under a unified pruning budget.

InternVL2. InternVL2 [10] is a high-resolution model, employing a dynamic high-resolution strategy by dividing images into 448×448 tiles, with aspect ratios matched from a predefined set to retain natural proportions, it scales up to 40 tiles to accommodate 4K resolution. A 448×448 thumbnail of the entire image is included alongside the tiles to provide global context. Pixel shuffling reduces each 448×448 tile to 256 visual tokens, enabling efficient high-resolution processing with a reduced token count. Since multiple sub-images tiles are directly inputted into the model for pro-

cessing, we restore each sub-image to a two-dimensional arrangement and then perform AdaptPrune under a unified pruning budget. In our AdaptPrune, each sub-image is processed individually. During AdaptPrune token selection, we consider scores across all tokens but ensure that the adaptive suppression process does not cross sub-image boundaries.

B. Datasets

To demonstrate the broad applicability of our approach, we use several representative datasets that cover a wide spectrum of task domains for evaluation, including Image Captioning, General Visual Question Answering, Text-based Visual Question Answering, and Multimodal Reasoning.

Image Captioning. In Image Captioning, models generate a descriptive sentence for each image. We use the Nocaps [1] and Flickr30K [40] datasets as benchmarks. Nocaps [1] is the first large-scale benchmark dataset featuring 166,100 human-generated captions for 15,100 images, designed to evaluate image captioning on novel objects. The Flickr30k [40] dataset is a standard benchmark for sentence-based image description, featuring 31,000 images, each accompanied by five reference sentences provided by human annotators. We prompt the model with the phrase "Provide a one-sentence caption for the provided image." for both benchmarks and use the CIDEr score [48] for measurement metric.

General Visual Question Answering. Visual Question Answering (VQA) requires the model to generate an answer for a given image-question pair based on the content of the image. We evaluate the model's performance on four commonly used and representative datasets: VQAv2 [18], OK-VQA [36], VizWiz [19], and GQA [22]. VQAv2 [18] is a manually annotated open-ended question and answer dataset about images, requiring an understanding of visuals, language, and common sense to answer the questions. OK-VQA [36] is a benchmark for knowledge-based visual question answering, featuring over 14,000 questions that require external knowledge to answer, designed to challenge current VQA models and encourage the integration of external data sources. VizWiz [19] dataset consists of images and spoken questions from blind users, each with 10 crowdsourced answers, challenging models to predict answers or identify unanswerable questions. GQA [22] is a visual question answering dataset featuring real images with balanced Q&A pairs, scene graph annotations, and pre-extracted visual features from advanced detection models. The model is prompted with the instruction: "Answer the question using a single word or phrase." for all benchmarks.

Category (dev)	LLaVA-1.5-7B [29]	FastV [9] 90%	AdaptPrune 90%	FastV [9] 75%	AdaptPrune 75%
Action Recognition	90.7	85.2	88.9	87.0	90.7
Attribute Comparison	50.0	50.0	54.5	52.3	54.5
Attribute Recognition	79.7	68.9	75.7	77.0	79.7
Celebrity Recognition	79.8	76.8	74.7	78.8	78.8
Function Reasoning	75.9	72.2	70.9	75.9	70.9
Future Prediction	45.0	30.0	37.5	40.0	42.5
Identity Reasoning	93.3	86.7	95.6	95.6	97.8
Image Emotion	78.0	58.0	78.0	78.0	76.0
Image Quality	35.8	22.6	30.2	28.3	32.1
Image Scene	96.2	90.4	94.2	96.2	97.1
Image Style	77.4	73.6	71.7	77.4	77.4
Image Topic	83.3	80.6	83.3	83.3	83.3
Nature Relation	41.7	39.6	37.5	37.5	37.5
Object Localization	39.5	35.8	38.3	37.0	38.3
OCR	59.0	59.0	59.0	59.0	59.0
Physical Property Reasoning	50.7	53.3	49.3	53.3	50.7
Physical Relation	33.3	41.7	41.7	41.7	41.7
Social Relation	88.4	53.5	55.8	72.1	69.8
Spatial Relationship	17.8	17.8	17.8	17.8	17.8
Structured Image-Text Understanding	26.9	30.8	26.9	28.2	26.9

Table 6. MMBench [33] finegrained comparison between FastV and AdaptPrune at 90% and 75% pruning ratios.

We use exact match accuracy as the metric for measurement.

Multimodal Reasoning. Multimodal reasoning demands more sophisticated perception, knowledge, and reasoning skills than VQA, which makes it a more comprehensive task for evaluating the integrated capabilities of LVLMs. We assess these skills with the datasets MME, MMBench [33], and POPE [25]. MMBench [33] is a systematically designed benchmark for evaluating LVLMs, offering a diverse set of multi-choice questions, rigorous quality control, and a unique CircularEval strategy to ensure accurate and holistic model assessments. MME is a comprehensive evaluation benchmark for LVLMs, designed to assess their perception and cognition abilities across 14 sub-tasks, with manually crafted instruction-answer pairs to ensure a fair comparison and minimize data leakage. POPE [25] is an innovative evaluation method designed to more effectively and flexibly assess object hallucination in large vision-language models by utilizing a polling-based query approach. The model is prompted with the instruction: "Answer the question using a single word or phrase." for MME. The model is prompted with the instruction: "Answer with the option's letter from the given choices directly." for MMBench [33]. We use accuracy as the metric for MME and POPE [25] and GPT Evaluation Score by GPT-3.5-Turbo-0613 as the metric for MMBench [33].

Text-based VQA. Text-based visual question answering focuses on understanding textual information within images. We evaluate this capability with the datasets TextVQA [45], DocVQA [38], and ChartQA [37]. The TextVQA

[45] dataset focuses on visual question answering in scene text scenarios, challenging models to read and interpret text within images to answer related questions. The DocVQA [38] dataset offers 50,000 questions across over 12,000 document images, challenging models to understand document structure and content for Visual Question Answering. ChartQA [37] is a large-scale benchmark with over 32.7K questions, combining human-written and generated queries from chart summaries, designed to test complex visual and logical reasoning on charts. The model is prompted with the instruction: "Answer the question using a single word or phrase." for all benchmarks. We use exact match accuracy as the metric for TextVQA [45] and ChartQA [37] and ANLS Score as the metric for DocVQA [38].

C. Pruning Strategy Ablation

We conduct a series of ablation studies on our pruning strategy with comparison methods commonly used in other works [7, 9, 55]. Our experiments include: (a) a single-layer implementation of FitPrune, which uses the cross attention between image and text multiplied by the self attention among image tokens; (b) selecting every other token from the top 20% tokens; (c) randomly selecting 10% tokens from all image tokens; (d) randomly selecting one token from each 3x3 grid and then choosing the top 10% tokens; (e) selecting the highest scoring token from each 3x3 grid, and then choosing the top 10% tokens; (f) applying average pooling with a stride of 1 and a kernel size of 3 over the two-dimensional image; (g) selecting the last 10% of the

L2-category (dev)	LLaVA-1.5-7B [29]	FastV [9] 90%	AdaptPrune 90%	FastV [9] 75%	AdaptPrune 75%
Attribute Reasoning	70.4	68.3	68.3	71.9	69.3
Coarse Perception	77.4	68.6	74.7	76.0	76.7
Finegrained Perception (Cross-Instance)	55.2	53.1	55.9	54.5	56.6
Finegrained Perception (Instance-Level)	65.9	61.1	62.8	64.2	65.2
Logic Reasoning	33.1	30.5	30.5	32.2	32.2
Relation Reasoning	57.4	45.2	45.2	51.3	50.4

Table 7. MMBench [33] L2-category finegrained comparison between FastV and AdaptPrune at 90% and 75% pruning ratios.

Category	LLaVA-1.5-7B [29]	FastV [9] 90%	AdaptPrune 90%	FastV [9] 75%	AdaptPrune 75%
Code Reasoning	67.5	45.0	62.5	70.0	52.5
Numerical Calculation	70.0	47.5	57.5	52.5	55.0
Text Translation	107.5	125.0	117.5	120.0	115.0
Commonsense Reasoning	112.9	111.4	112.9	120.0	117.1
Artwork	119.5	106.5	113.8	120.0	117.5
Celebrity	137.1	127.4	133.2	138.5	134.7
Count	155.0	95.0	138.3	143.3	145.0
Color	170.0	130.0	155.0	170.0	170.0
Position	128.3	86.7	115.0	130.0	126.7
OCR	140.0	125.0	125.0	147.5	132.5
Landmark	163.8	136.5	154.0	157.5	166.0
Scene	158.0	147.5	165.8	159.8	163.3
Existence	190.0	135.0	165.0	160.0	170.0
Posters	146.6	128.2	144.9	142.5	149.3

Table 8. MME finegrained comparison between FastV and AdaptPrune at 90% and 75% pruning ratios.

image token sequence. The experiment results demonstrate that our method is the most effective.

D. Finegrained Results

D.1. MMBench Finegrained Results

As shown in Table 6, in the MMBench [33] fine-grained comparison between FastV [9] and AdaptPrune at 90% and 75% pruning ratios, significant performance improvements are evident with AdaptPrune in several categories. Specifically, AdaptPrune shows enhanced outcomes in Action Recognition, Attribute Recognition, Future Prediction, Identity Reasoning, Image Emotion, Image Quality, and Image Scene. These results underline AdaptPrune’s ability to retain crucial visual information for complex understanding and response capabilities within dynamic environments.

The MMBench [33] L2-category comparison in Table 7 reveals that AdaptPrune generally improves performance in categories such as Coarse and Finegrained Perception. This indicates that AdaptPrune’s nuanced pruning approach could be beneficial for detailed perceptual analysis.

D.2. MME Finegrained Results

In the MME comparison in Table 8, AdaptPrune’s strategy demonstrates considerable success in categories includ-

ing Code Reasoning, Commonsense Reasoning, Artwork, Count, Color, Position, Landmark, Scene, Existence, and Posters. These improvements suggest that AdaptPrune is particularly effective in contexts requiring an intricate understanding of visual and contextual elements, arguably due to its capability to preserve essential tokens that encapsulate critical information for interpreting complex scenarios.

E. Visual Attention Distribution

In Figure 8 and Figure 9, we present the average attention score distribution across each layer of LLaVA-1.5-7B. We randomly choose 1,000 samples from the VQAv2 [18] benchmark of the General VQA task and the MMBench [33] benchmark of the Multimodal Reasoning task for analysis. The model exhibits an almost identical attention distribution pattern for image tokens within the same layer, even though these samples come from entirely different tasks. The pattern changes slightly across different layers, the pattern changes slightly, but some of the tokens receiving the highest attention remain consistent. The detailed statistical results further reveal that the model’s attention scores exhibit specific positional bias.

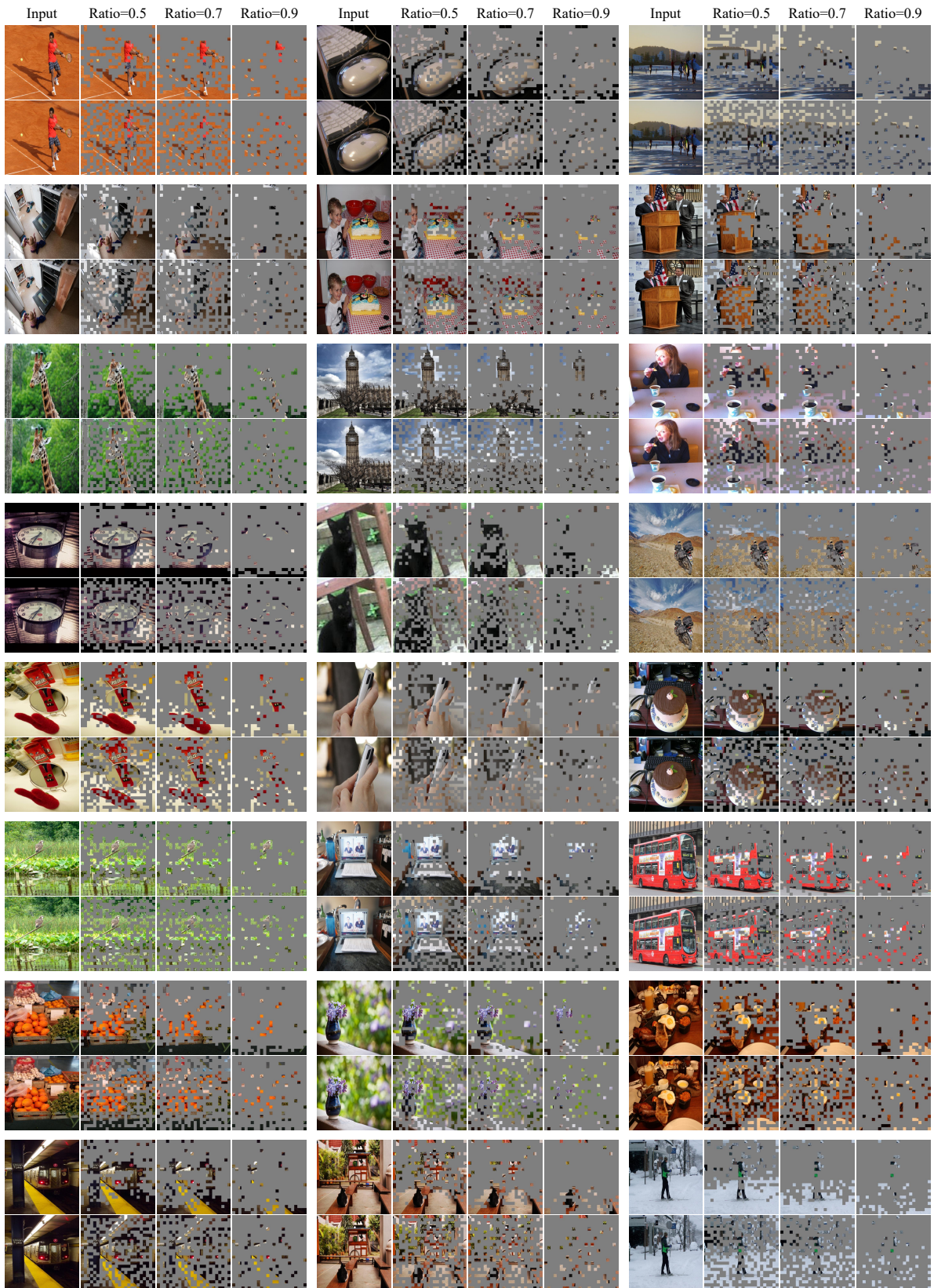


Figure 7. Uncurated random sample comparison on VQAv2 [18] benchmark images. For each comparison group with 8 images, the top row shows FastV [9] results and the bottom row shows AdaptPrune results, with columns from left to right for input images and pruning ratios of 0.5, 0.7, and 0.9.

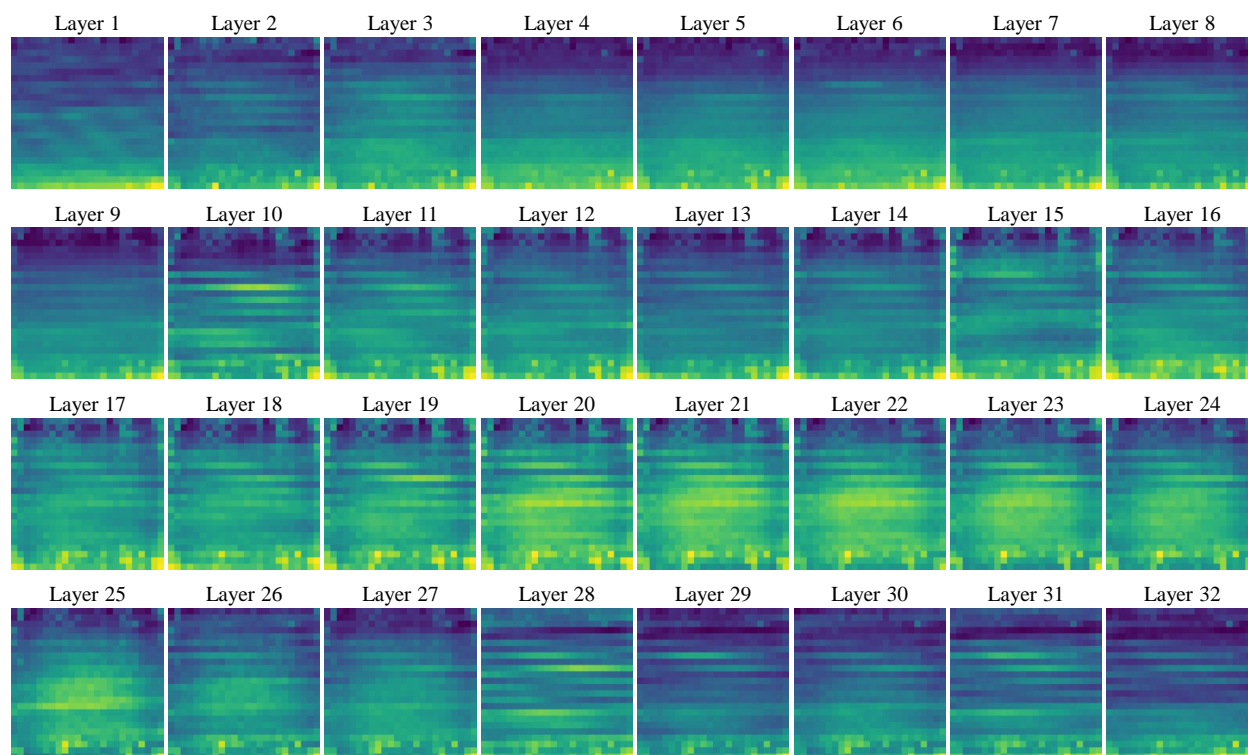


Figure 8. Visualization of the average attention distribution across each layer of LLaVA-1.5-7B. The attention scores are computed from 1,000 random samples of VQAv2 [18].

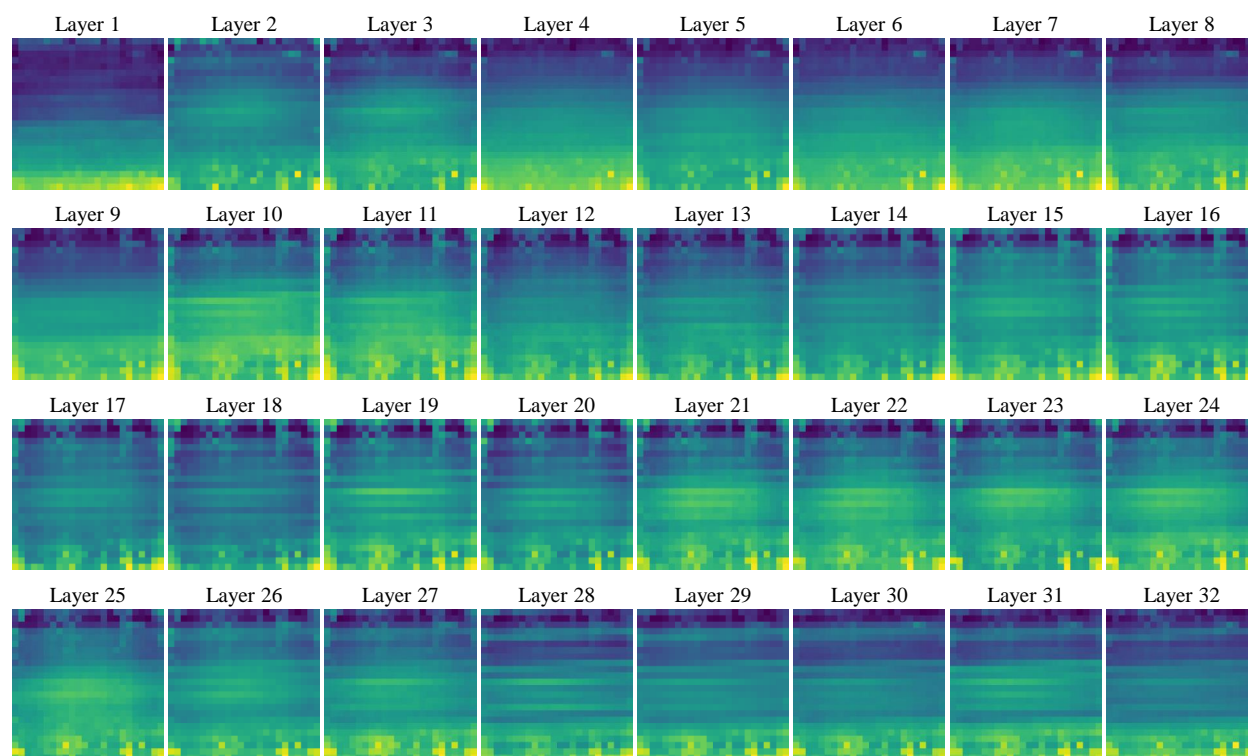


Figure 9. Visualization of the average attention distribution across each layer of LLaVA-1.5-7B. The attention scores are computed from 1,000 random samples of MMBench [33].